Phase synchronization of a pair of spiral waves

Meng Zhan,[1,2,*] Xingang Wang,[1] Xiaofeng Gong,[1] and C.-H. Lai[3]
[1]*Temasek Laboratories, National University of Singapore, 117508 Singapore*
[2]*Chemical Physics Theory Group, Department of Chemistry, University of Toronto, Toronto, Ontario, Canada M5S 3H6*
[3]*Department of Physics, National University of Singapore, 117542 Singapore*
(Received 11 October 2004; revised manuscript received 6 January 2005; published 18 March 2005)

The interaction of a pair of spiral waves with different independent rotation frequencies is studied. In a very large frequency mismatch searching region, we observe three different pattern formation phenomena: (a) phase-synchronization-induced invasion under a relatively small frequency mismatch, i.e., the spiral wave with slower frequency (longer period) is swept away by a traveling wave, which is induced and phase synchronized by the faster spiral wave; (b) the coexistence of two spiral waves at sufficiently large parameter mismatch; and (c) an intermediate state, a non-phase-synchronous invasion, that is, similarly the slower spiral wave is swept by an approximate planar wave, whose frequency, however, is intermediate between those of the faster and slower waves. A point-source model is studied to analyze all these phenomena in a unified way.

DOI: 10.1103/PhysRevE.71.036212 PACS number(s): 05.45.Xt, 47.54.+r

Spiral waves are probably the most intriguing patterns in spatially extended systems [1–5]. They have been observed in diverse systems, including biological systems (such as the cardiac muscle tissue and aggregating slime-mold cells), physical systems (such as CO oxidation on platinum), and the chemical Belousov-Zhabotinsky reaction, etc. Spiral waves have been actively investigated for several reasons, one of which is their potential clinical relevance to cardiac arrhythmias, especially ventricular fibrillation, which can induce clinical death in only one minute and is the leading cause of sudden heart death in industrialized countries. In general, most studies in these fields are focused on the formation mechanisms, the instability of spiral waves (meandering spirals, or different breakup scenarios) [6–8], the response of spiral waves under all kinds of external perturbations [9–11], such as the modulation by a periodic force pulse, local (and global) feedback, electric fields, and noise, and the interactions of spiral waves (pattern selection). Clearly the motivations of all of these studies are closely connected with the possible application and control of spiral waves [10,11].

A specific question about the interaction of multiple spiral waves—what will happen if several spiral waves are put into one spatial domain—has aroused great interest continuously in the pattern formation community [12–23]. It is a basic question and is also of significance in our understanding of spiral wave formation in chemical medium, cardiac tissue, etc. Until now, it has been well accepted that the interaction between several spiral waves with different frequencies often leads to the conversion of the slower spiral wave to the faster frequency, and, thus, the domination of the fastest spiral wave in the whole space. This pattern has been extensively observed in various systems, such as an active chemical medium [17], a two-dimensional excitable medium with a parameter gradient [19], self-interactions of a scroll ring in three dimensions [19], and cardiac tissue [22]. More specifically, two distinct phases of the interaction including unwinding and drifting states have been observed [19]. Initially, the spiral with the faster rotation period intrudes (unwinds) into the domain of the slower one; after the unwinding, the wave fronts from the faster spiral interact directly with the center of rotation of the slower one, producing a drifting of the slower one to move out of the observed domain. Therefore, the unwinding (or invading) velocity and the drifting speed are the two most important characteristics in the interactions. In an early seminal paper [17], Krinsky and Agladze pointed out that the underlying mechanism of the invasion is due to the (phase) synchronization of autowave sources (spiral waves); that is, the spiral with the faster frequency can cause the region in the vicinity of the interaction to be excited with its frequency, i.e., (phase) synchronized, and then the action keeps on expanding to the entire region. As a result, spiral waves with unequal frequencies cannot coexist and the most rapid one survives. This point of view has successfully explained the observed phenomena and a point-source model based on this argument also approximately gives a formula for the unwinding time. Recently, the effect of weak inhomogeneity on spiral wave dynamics was studied within the framework of the two-dimensional complex Ginzburg-Landau equation description in a quasifrozen parameter region [20,21]. Just as in an excitable medium, the formation of a dominant spiral domain that suppresses other spiral domains was observed in this type of oscillatory medium.

Until now, to our knowledge, most studies only focused on observations with small frequency mismatch, or weak inhomogeneity, for example, the maximum frequency difference ratio is within a factor of 20% in Ref. [20]. Hence, some interesting questions involving the interaction of spiral waves are still not answered: What will happen if the frequency mismatch is very large? Can one spiral wave destroy another as long as its frequency (period) is larger (smaller)? Is phase synchronization the unique mechanism for the faster spiral destroying the slower one? In this paper, we intend to address these problems.

*Electronic address: mzhan@chem.utoronto.ca

Our studies are based on the two-dimensional complex Ginzburg-Landau equation (CGLE),

$$\frac{\partial A}{\partial t} = \mu(x,y)A - (1+i\alpha)|A|^2A + (1+i\beta)\nabla^2 A, \qquad (1)$$

which provides a universal description of extended systems in the vicinity of a homogeneous Hopf bifurcation with the complex variable $A(x,y,t)$ being the order parameter at the bifurcation [1,5,20]. In the case of a homogeneous medium, α and β are real constants. It is well known that in an appreciable region of the (α,β) parameter space, a spiral wave can naturally form from fairly arbitrary small initial perturbations from $A=0$. Here the scaling parameter μ is chosen as a real constant, and it can be set to unity by an appropriate rescaling of Eq. (1) [20] through $x\to x/\sqrt{\mu}$, $t\to t/\mu$, $A\to\sqrt{\mu}A$. Directly we have the scaling relation for the two system characteristics: the rotation frequency and the wavelength of the spiral waves,

$$\omega(\mu) = \mu\omega_0,$$

$$\lambda(\mu) = \lambda_0/\sqrt{\mu}, \qquad (2)$$

where ω_0 and λ_0 are for a single spiral wave at $\mu=1$ with $\omega(\mu)$ and $\lambda(\mu)$ for arbitrary μ, correspondingly. For system (1), it is easy to derive the dispersion relation including μ,

$$\omega(\mu) = \alpha\mu + (\beta-\alpha)k(\mu)^2, \qquad (3)$$

where $k(\mu)$ is the wave number of a planar wave [1,2,20].

It has been pointed out that the lowest order effect of the inhomogeneity is the dependence of the local frequency and growth rate of excitation on space [20]. In the present work, a simple model is constructed with two stable spiral waves having different scaling parameters in the left and right sides of the domain, namely, $\mu(x,y)=\mu_l$ for $x\leqslant L$, and $\mu(x,y)=\mu_r$ for $x>L$ with the size of the medium $L_x=2L$ and $L_y=L$. In this rectangular region, the interaction of two parallel spirals will be investigated. Without losing any generality, $\alpha=-0.4$ and $\beta=-1.5$, which are the typical values in the normal outwardly rotating spiral wave region [5,24,25], are chosen. In this paper, we mainly study systems with the variation of μ_r and a fixed left scaling parameter $\mu_l=3$. The CGLE system is integrated using the explicit Euler method with time step $\Delta t=0.01$, and the standard five-point approximation for the Laplacian operator with the space step $\Delta x=\Delta y=0.5$. For each spiral wave, a 256×256 grid with no-flux boundaries is utilized. The main computation procedure is to form two stable spiral waves in the individual regions first, which can be conveniently realized by vertically intersecting initial conditions, and then to remove the obstacle in the middle of the computation domain and switch the interaction on. Our model here is constructed to maintain simplicity and generality, so the results in this paper are expected to be applicable to other more complex systems as well.

As a first example, $\mu_r=3.5$, only a little larger than $\mu_l=3$, whose evolutions are depicted in Fig. 1, is selected. In the initial time [Fig. 1(a)], two separated spiral waves spontaneously form and the division between is quite even. In the course of time, we observe that the right spiral wave excites

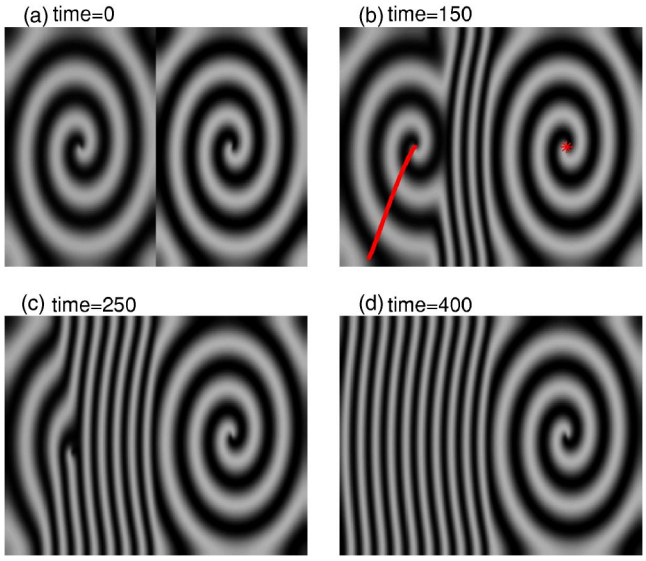

FIG. 1. The time evolution of $\mathrm{Re}[A(x,y)]$ at $\mu_r=3.5$. $\mu_l=3$ is fixed throughout this paper.

a traveling wave (approximate planar wave) with a fixed wavelength, which is discernibly different from both the left and right original spiral waves. Two processes of the interaction are very clear: unwinding [Fig. 1(b)] and drifting [Fig. 1(c)]. In these figures, the tip trajectory of the left spiral is indicated by a solid line, whereas the nearly quiescent tip of the right spiral is denoted by stars. Ultimately, a stable pattern is established, characterized by the slower spiral being completely transformed to a traveling wave [Fig. 1(d)].

The above reconfirms the observation that spiral waves with unequal frequencies cannot coexist. We also compute the eventual rotation frequencies of the left and right regions having uniform values, denoted, respectively, by solid circle and open square points in Fig. 2(a), as a function of $\mu(r)$. Figures 2(b)–2(d) are three enlarged fields focusing on the specific regions. Actually, due to the regular motion of the coupled sites, periodic or quasiperiodic, these are very easy to measure. Here, we borrow a mature technique in the field of chaotic phase synchronization [26–28] and define the average frequency (rotation number) of the spatial integration points as

$$\omega(x,y) = \left\langle \frac{d\theta(x,y)}{dt} \right\rangle = \lim_{T\to\infty} \frac{1}{T}\int_0^T \theta(\dot{x},y)dt \qquad (4)$$

based on the phase definition of

$$\theta(x,y) = \arctan\left(\frac{\mathrm{Im}[A(x,y)]}{\mathrm{Re}[A(x,y)]}\right), \qquad (5)$$

where $\mathrm{Re}[A(x,y)]$ and $\mathrm{Im}[A(x,y)]$ are the real and imaginary parts of $A(x,y)$, respectively. The counterclockwise direction is viewed as the normal positive rotation. For regular rotation of each computation point with a single cycling center as analyzed in this paper, it works well. It has been mentioned that the presence of a topological defect (the spiral core) does not pose any problems because the defect, whose phase is not defined though, is located almost surely between the in-

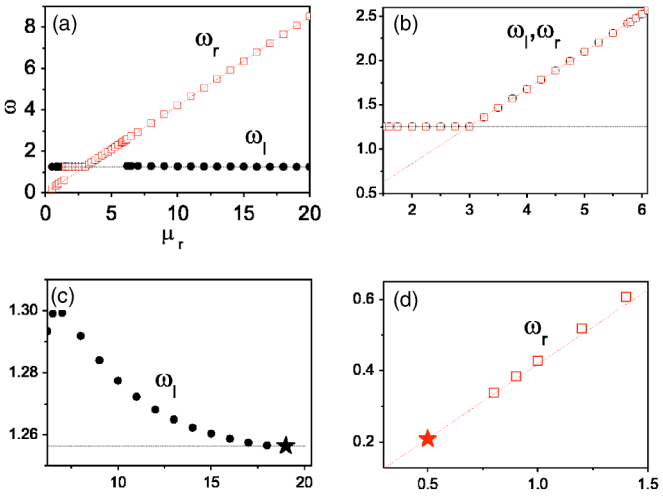

FIG. 2. (a) The two end frequencies of the left and right sides in the pattern, ω_l (solid circles) and ω_r (transparent squares) versus μ_r. (b), (c), and (d) Three enlargements of (a). In (b), the quantities of ω_l and ω_r coincide, which means the global phase synchronization has been established. In (c) and (d), non-phase-synchronization appears with $\omega_l \neq \omega_r$. However, the wave invading phenomena have still been observed as the frequency of the invading wave is a little larger than that of the invaded spiral wave. The two critical values (stars) of (a) are at the right side, $\mu_r=19.0$ (c), and the left one, $\mu_r=0.5$ (d).

tegration lattice sites [28]. In fact, $\omega(x,y)$ of a single spiral with homogeneous parameter sets shows the same single magnitude with, however, the different sign as the spiral frequency of $\omega(\mu)$ [in Eq. (3)].

Figure 2(b) clearly shows that in the region of $1.5 \leqslant \mu_r \leqslant 6.1$, the frequencies of the two spatial parts coincide, i.e., global phase synchronization has been established. In particular, the end frequency of the coupled systems is decided by the large one, and we see a huge jump not only in the region of $3=\mu_l<\mu_r \leqslant 6.1$, but also in $3=\mu_l>\mu_r \geqslant 1.5$. Note that, for $\mu=1$, $\omega_0=0.4188$, the dashed lines indicate the initial frequencies, the frequencies for the individual spiral waves without coupling, which are located at $\omega_l=\mu_l\omega_0=3\omega_0$ and $\omega_r=\mu_r\omega_0$, respectively.

Now we may ask, what will occur if μ_r stays out of the phase synchronization region? With a similar qualitative behavior as Fig. 1, two phases of interaction, unwinding [Fig. 3(b)] and drifting [Fig. 3(c)], are exemplified for $\mu_r=8.0$. Because of the large discrepancy of the two scaling parameters, the differences of the wavelengths and the variable magnitudes (different gray values) between the two sides are visible. In the end, the systems are built with two components of patterns: the unchanged right spiral wave and an approximate planar wave on the other side [Fig. 3(d)]. According to the non-phase-synchronous feature in Fig. 2(a), $\omega_r \neq \omega_l$ for $\mu_r=8.0$, it seems very strange that the stable traveling wave pattern in Fig. 3 is still possible. A closer look [see Fig. 2(c) at $6.2 \leqslant \mu_r < 19.0$ and Fig. 2(d) at $0.5<\mu_r \leqslant 1.4$] clearly indicates that although the chosen frequency of the invading wave is different from that of the faster spiral, it is still a little larger than that of the slower one, which will be invaded (dots are located above the dashed lines in both subfigures). The two stars labels the two critical parameters.

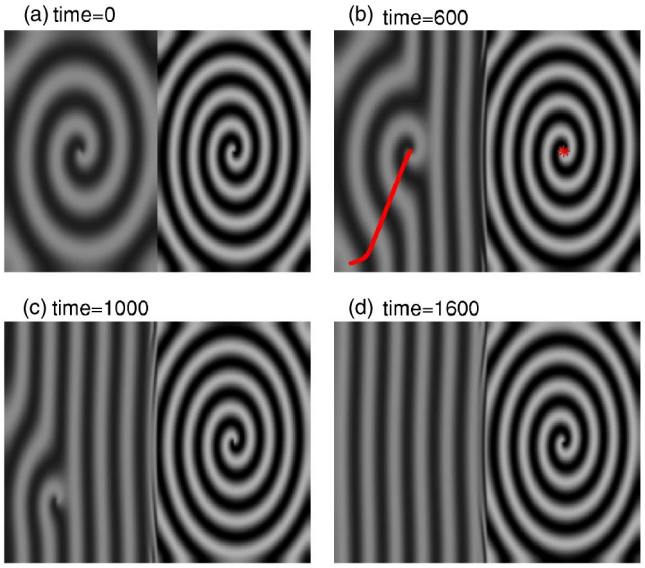

FIG. 3. Similar to Fig. 1 at $\mu_r=8.0$.

So far we know that the frequency of the induced invading wave is crucial for its occupation of the slower spiral domain. Several stable patterns for larger frequency differences, $\mu_r=19.0$ for Fig. 4(a) and $\mu_r=0.5$ for Fig. 4(b), clearly confirm this point. Although the frequency difference is so large and the intermediate region is so greatly influenced by the coupling, two spiral waves definitely coexist and the induced wave front with the larger frequency cannot expand in the new territory. It should be stressed that here an extremely long observation time 80 000 (comparatively one or two orders of magnitude longer than in Figs. 1 and 3) has been adopted. Similar phenomena are found for much larger $\mu_r(\mu_r>19.0)$ or smaller $\mu_r(\mu_r<0.5)$. On the contrary, other stable patterns with different $\mu_r, \mu_r=1.0$ [Fig. 4(c)] and μ_r

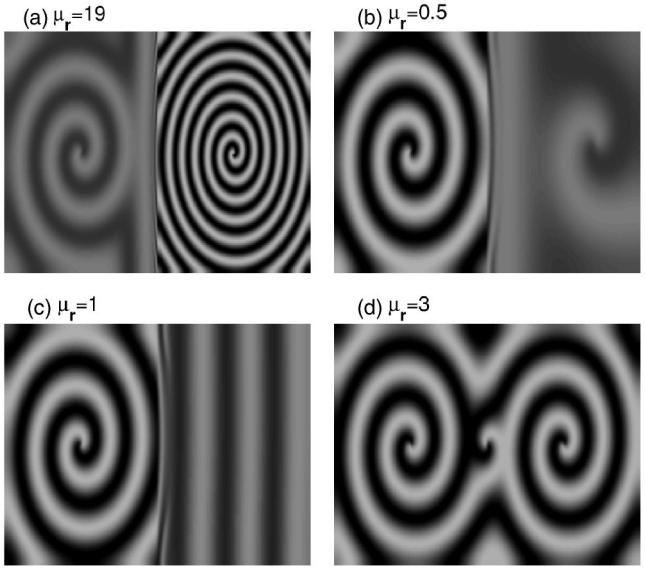

FIG. 4. The eventual stable patterns for different parameters: $\mu_r=19$ (a), 0.5 (b), 1.0 (c), and 3 (d).

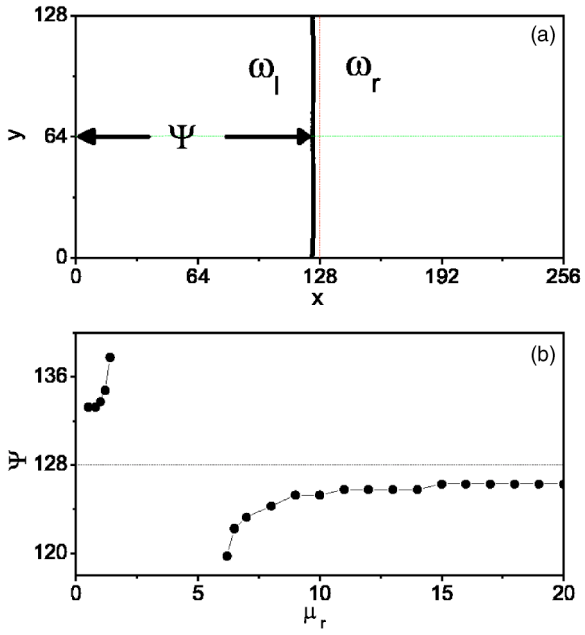

FIG. 5. (a) The frequency division line for two asymptotic frequencies ω_l and ω_r at $\mu_r=8$ [Fig. 3(d)]. In fact, it is a curve. At each side, $\omega(x,y)$ has a homogeneous value. Specifically, the intersection position of the division line with $y=L/2=64$, Ψ, is chosen. Under this parameter $\mu_r>\mu_l$, the division line has been moved into the slow spiral domain; thus $\Psi<L$. (b) The divided position Ψ vs μ_r.

$=3.0$ [Fig. 4(d)], show the left spiral wave (still faster) killing the right spiral and the coexistence of two spiral waves with the same frequencies ($\mu_r=\mu_l=3.0$), respectively. The appearance of a new small spiral wave near the center in Fig. 4(d) is simply due to the topological defect between the two initial spirals.

It should be highlighted here that the values of ω_l and ω_r in Fig. 2 are the two asymptotic quantities of $\omega(x,y)$ in the left and right sides, in which $\omega(x,y)$ has nearly uniform values. As an example, the frequency division line under $\mu_r=8$ [Fig. 3(d)] is exhibited in Fig. 5(a). It is a curve now and it has shifted from the middle vertical dash line, $x=L=128$, into the slow spiral wave domain. Specifically, the intersection position of this line with $y=L/2=64$, Ψ, is chosen, whose relation with μ_r is displayed in Fig. 5(b). Unlike in global phase synchronization (homogeneous in the whole domain and without a division) in the phase-locking region, a small expansion of the faster spiral to the slower one (deviation from the original division dashed line at $x=L=128$) is seen everywhere even including the coexistence state region. This indicates that, weaker than the global synchronization, partial synchronization, characterized by a two-value distribution (homogeneous in each part) and the extension of the large frequency field, is established out to the phase-locking region.

The stable patterns at different μ_r tell us that frequency locking is only a sufficient condition, not a necessary one, for the formation of the invading wave. More generally, even if the frequency of the induced invading wave is only a little bit higher than that of the slower spiral (not synchronous with the faster one), the expansion of the planar wave is still

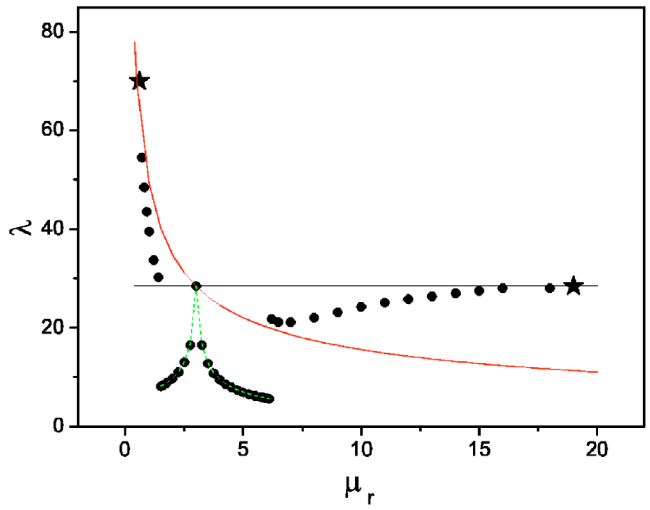

FIG. 6. The wavelength of the invading wave versus μ_r.

possible. It is useful to illustrate this by studying the wavelength of the established invading wave, shown by solid circles in Fig. 6. The two solid lines are the theoretical values for λ_l and λ_r without coupling. Here, $\lambda_0=49.25$, $\lambda_l=\lambda_0/\sqrt{3}=28.44$, and $\lambda_r=\lambda_0/\sqrt{\mu_r}$. In the synchronization region, the wavelength of the invading wave λ_i is smaller than both λ_r and λ_l (except for the extreme point $\mu_r=\mu_l=3.0$, $\lambda_i=\lambda_r=\lambda_l$, where the formation of invading wave is not possible). In fact, with the phase synchronization mechanism ($\omega_r=\omega_l$), it is easy to predict the wavelength of the induced planar wave through the dispersion relation [Eq. (3)]—this is shown as the dashed line, which fits the computational results very well. It is well known that the minimum wavelength $\lambda_{\min}$ (or maximum frequency) sustained by a specific medium to emit a wave is determined by the system parameters. Here indeed $\lambda_{\min}$ also controls the synchronization width (the phase-locking parameter range). Outside of the synchronization region, the stable invading wave appears with a new aspect of wavelength, i.e., λ_i is larger than that of the faster spiral wave and smaller than that of the slower one. Two extreme values are $\mu_r=19.0$($\mu_r=0.5$) in the right (left) side (stars in Fig. 6). Here we should mention that for some other parameter sets [different (α,β)], two phases without non-phase-synchronous invasion have also been found. In principle, the reason is that the coupled system does not have enough parameter range for μ_r in the synchronization region to arrive at $\lambda_{\min}$ under the current competition status between the growth power (μ), the strength of the local nonlinearity (α), and the intensity of the spatial coupling (β).

From the above discussion, we have obtained a clear physical picture of the interaction between the two spiral waves. To proceed further, it is crucial to investigate the invading velocity quantitatively. Actually for an approximate analysis with a point-source model [17] it has been derived with the form

$$V=v(1-T_1/T_2)/2, \tag{6}$$

where $T_1<T_2$ are the periods of the spiral waves, and v is the wave velocity. Obviously the wave velocities in different

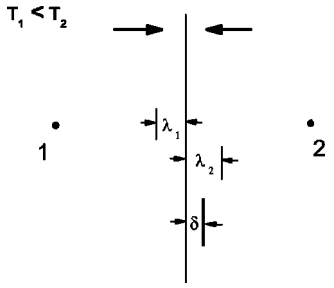

FIG. 7. Diagram of the point-source model.

media are not distinguished. Recently, in studies of several spiral waves in the quasifrozen parameter region, the relationship of the domain wall velocity (the same as the invading velocity in our paper) is given [20] by

$$V = (\omega_1 - \omega_2)/(k_1 + k_2), \tag{7}$$

where ω_1 and ω_2 are the spiral frequencies, k_1 and k_2 are the wave vectors, and the reference positive direction points toward spiral 2. If the discrepancy between k_1 and k_2 is not considered, Eq. (6) is recovered from Eq. (7) naturally.

We now know that a frequency difference of the spiral waves cannot always induce the invasion. Thus, the expressions in both (6) and (7) cannot explain the observations in the entire parameter region. Here we restudy a point-source model with the sketch map shown in Fig. 7. Just as in Ref. [17] and the numerical experiment above, two spiral waves are generated at the left and right sides, and $T_1 < T_2$. The essential point in the point-source model is that the two spiral waves can be simplified as two-point sources situated at the tip points 1 and 2, respectively, with emissions of planar waves having the same wavelength and frequency as the spiral waves. Indeed, if the two sources emit a first wave simultaneously, these waves will collide and annihilate midway between the sources, illustrated as two wave fronts with different wavelengths λ_1 and λ_2 colliding in the middle at the starting time of the interaction in Fig. 7. The point of the wave collision by the next two wave fronts will be shifted by δ toward the right side (the slower source) because $T_1 < T_2$. Thus, the question of the determination of the invading velocity is reduced to that of calculating the moving speed of the wave collision points. More importantly, after some short transient time, the expansion velocity should be decided by the competition of the right spiral wave and the traveling wave (not the left spiral wave).

Therefore we have

$$\delta = \lambda_2 - v_2 t = v_2(T_2 - t),$$

$$\delta = v_i t - \lambda_i = v_i(t - T_i), \tag{8}$$

where δ is the moving distance of the wave collision in time interval t, and v_i is the wave velocity of the invading wave. It should be emphasized that v_i is different from (and much larger than) V. Combining Eqs. (8) with $V = \delta/t$, we have

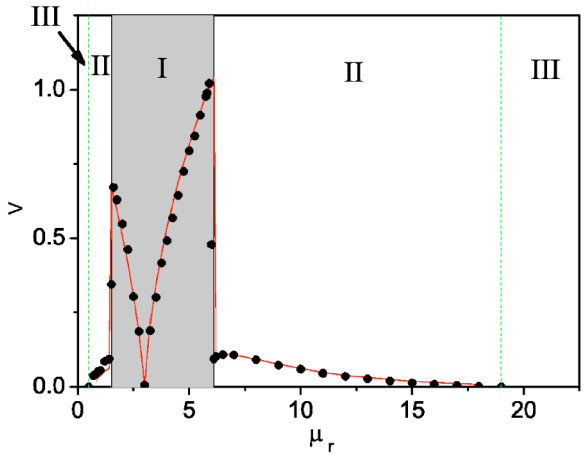

FIG. 8. The invading velocity V vs μ_r. The numerical result (solid points) fits with the theoretical analysis from Eq. (9) (solid line) very well. Three types of dynamic behaviors are classified as I, II, and III, corresponding to the phase-synchronized invading, non-phase-synchronized invading, and coexistence, respectively.

$$V = (\omega_i - \omega_2)/(k_i + k_2), \tag{9}$$

where ω_i and ω_2 are the rotation frequencies of the invading wave and spiral 2; k_i and k_2 are the wave numbers. The only difference from Eq. (7) is that now the information of the invading wave must be included. In fact, ω_i and k_i are not independent; they are linked by the dispersion relationship [Eq. (3)]. Even with synchronization $\omega_i = \omega_1$, the expression is still different from Eq. (7) ($k_i \neq k_1$); without synchronization, ω_i is determined by the coupling systems and can only be obtained numerically. A direct outcome from Eq. (9) is that the necessary condition for the formation of an invading wave is $\omega_i > \omega_2$, not $\omega_1 > \omega_2$; whereas if $\omega_i = \omega_2$, the spiral waves coexist.

To check the above results, the invading velocity V (mag-

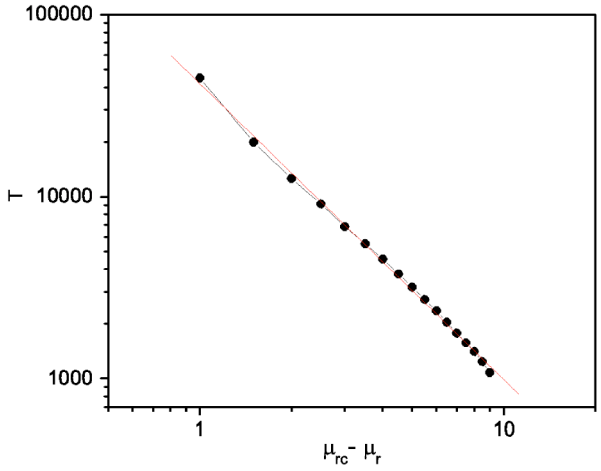

FIG. 9. Log-log plot of T vs $\mu_{rc} - \mu_r$. The power-law relationship between T and $\mu_{rc} - \mu_r$, i.e., $T \propto (\mu_{rc} - \mu_r)^{\beta}$, $\beta = -1.62 \approx -5/3$, and $\mu_{rc} = 19.0$, definitely confirms the coexistence behavior of a pair of spiral waves out of the non-phase-synchronization invading region.

nitude only) vs μ_r is studied in Fig. 8, where a solid line expressed by Eq. (9) fits very well with our direct numerical computation of $V=L/(2T)$, the solid circles. T is the time interval of the invading wave arriving at the tip of the slower spiral wave. Three distinct parts including the "V" shape of the V value in the phase synchronization region (filled in gray color and denoted by I), suddenly jumping to a relatively small value of V in non-phase-synchronization represented by II, and the damping to zero in the no-invading area indicated by III are clear. Another method with the computation of a short time local frequency variation also gives the similar results.

It is worth mentioning that the transition to the coexistence of a pair of spirals under sufficiently large frequency mismatch [like the two stars in Figs. 2(c) and 2(d)] does exist. To prove this point, in Fig. 9 the value of T near the critical parameter, for example, $\mu_r=19$, has been studied, and a fine scaling of $T\propto(\mu_{rc}-\mu_r)^{\beta}$ with $\beta=-1.62\approx-5/3$ and $\mu_{rc}=19.0$ has been found. For $\mu_r\geqslant\mu_{rc}=19.0$, T goes to infinity and the propagation of the invading wave into the new domain is not possible any more, although the frequency variation and the pattern disturbance in the slow spiral domain near the interaction boundary still happen [see Figs. 5(b), 4(a), and 4(b)].

In conclusion, many of the experimentally important media are inhomogeneous and the studies of two spiral waves in detail in the present work are significant. Some remarkable results of this study are as follows.

(1) In the entire frequency mismatch space, three different kinds of pattern formation including phase synchronization induced invasion, non-phase-synchronous invasion, and the coexistence of a pair of spirals, have been classified.

(2) The frequency discrepancy plays a dominant role in the interaction: phase locking is not the exclusive mechanism for the expansion of the invading wave and the frequency difference alone cannot guarantee the invasion of the faster spiral wave in space.

(3) A formula of the invading velocity from the point-source model can explain all these dynamic behaviors in a unified way.

All of the above results are robust and independent with the same (or opposite) chirality, and they can be simply extended to other cases of coupled antispiral waves [25]. Moreover, clearly the results in this paper are constructively helpful for the possible development of methods (or techniques) of the control of spiral waves. A specific example is that of spiral wave drifting induced by the stimulation of wave trains [29,30], which has been proposed recently as one possible alternative approach to the treatment of heart attack.

[1] M. Cross and P. Hohenberg, Rev. Mod. Phys. **65**, 851 (1993).
[2] Y. Kuramoto, *Chemical Oscillations, Waves, and Turbulence* (Springer-Verlag, New York, 1984).
[3] H. L. Swinney and V. I. Krinsky, *Waves and Patterns in Chemical and Biological Media* (MIT/North-Holland, Cambridge, MA, 1992).
[4] R. Kapral and K. Showalter, *Chemical Waves and Patterns* (Kluwer, Dordrecht, 1995).
[5] I. S. Aranson and L. Kramer, Rev. Mod. Phys. **74**, 99 (2002).
[6] M. Bar and M. O. Guil, Phys. Rev. Lett. **82**, 1160 (1999); M. Bar and L. Brusch, New J. Phys. **6**, 5 (2004).
[7] D. Barkley, Phys. Rev. Lett. **68**, 2090 (1992); Phys. Rev. Lett. **72**, 164 (1994).
[8] J. Yang, F. Xie, Z. Qu, and A. Garfinkel, Phys. Rev. Lett. **91**, 148302 (2003).
[9] V. S. Zykov, O. Steinbock, and S. C. Muller, Chaos **4**, 509 (1994).
[10] O. Steinbock, J. Schutze, and S. C. Muller, Phys. Rev. Lett. **68**, 248 (1992).
[11] S. Grill, V. S. Zykov, and S. C. Muller, Phys. Rev. Lett. **75**, 3368 (1995); V. S. Zykov, G. Bordiougov, H. Brandtstadter, I. Gerdes, and H. Engel, *ibid.* **92**, 018304 (2004).
[12] I. S. Aranson, L. Kramer, and A. Weber, Phys. Rev. E **47**, 3231 (1993).
[13] X. Zou, H. Levine, and D. A. Kessler, Phys. Rev. E **47**, R800 (1993).
[14] I. Aranson, H. Levine, and L. Tsimring, Phys. Rev. Lett. **76**, 1170 (1996).
[15] K. J. Lee, Phys. Rev. Lett. **79**, 2907 (1997).
[16] M. A. Bray and J. P. Wikswo, Phys. Rev. Lett. **90**, 238303 (2003).
[17] V. I. Krinsky and K. I. Agladze, Physica D **8**, 50 (1983).
[18] Y. A. Yermakova, V. I. Krinsky, A. V. Panfilov, and A. M. Pertsov, Biophysics (Engl. Transl.) **31**, 348 (1986).
[19] M. Vinson, Physica D **116**, 313 (1998).
[20] M. Hendrey, E. Ott, and T. M. Antonsen, Phys. Rev. Lett. **82**, 859 (1999); Phys. Rev. E **61**, 4943 (2000).
[21] T. Bohr, G. Huber, and E. Ott, Physica D **106**, 95 (1997); K. Nam, E. Ott, M. Gabbay, and P. N. Guzdar, *ibid.* **118**, 69 (1998).
[22] F. Xie, Z. Qu, J. N. Weiss, and A. Garfinkel, Phys. Rev. E **59**, 2203 (1999).
[23] F. Xie, Z. Qu, J. N. Weiss, and A. Garfinkel, Phys. Rev. E **63**, 031905 (2001).
[24] V. K. Vanag and I. R. Epstein, Science **294**, 835 (2001).
[25] Y. Gong and D. J. Christini, Phys. Rev. Lett. **90**, 088302 (2003); L. Brusch, E. M. Nicola, and M. Bar, *ibid.* **92**, 089801 (2004); Y. Gong and D. J. Christini, *ibid.* **92**, 089802 (2004).
[26] A. S. Pikovsky, M. G. Rosenblum, and J. Kurths, *Synchronization—A Unified Approach to Nonlinear Science* (Cambridge University Press, Cambridge, England, 2001).
[27] G. V. Osipov, B. Hu, C. Zhou, M. V. Ivanchenko, and J. Kurths, Phys. Rev. Lett. **91**, 024101 (2003).
[28] J. Davidsen and R. Kapral, Phys. Rev. E **66**, 055202 (2002).
[29] G. Gottwald, A. Pumir, and V. Krinsky, Chaos **11**, 487 (2001).
[30] A. T. Stamp, G. V. Osipov, and J. J. Collins, Chaos **12**, 931 (2002).